JOURNAL OF GEOPHYSICAL RESEARCH: OCEANS, VOL. 118, 5398–5411, doi:10.1002/jgrc.20404, 2013

Baroclinic M_2 tidal circulation in Algeciras Bay and its implications for the water exchange with the Strait of Gibraltar: Observational and 3-D model results

Carlos J. González,[1] Óscar Álvarez,[1] Rafael Mañanes,[1] Alfredo Izquierdo,[1] Miguel Bruno,[1] Juan J. Gomiz,[1] Jamal Chioua,[2] and Laura López[3]

Received 22 January 2013; revised 11 September 2013; accepted 18 September 2013; published 15 October 2013.

[1] The M_2 tidal circulation in Algeciras Bay (Strait of Gibraltar) is analyzed using a 3-D, nonlinear, baroclinic, hydrodynamic model, in conjunction with observed data series. Results show the influence of the density stratification on the vertical structure of the M_2 currents in Algeciras Bay, although its tidal dynamics shows major differences with respect to the Strait of Gibraltar. Whereas the M_2 currents in the Strait present mainly barotropic behavior, the baroclinic effects prevail in Algeciras Bay. A notable finding is the presence of a tidal M_2 counter-current system between the upper Atlantic and the lower Mediterranean water layers within the Bay, with amplitudes of up to 25 cm s^{-1}. The interface between the two layers oscillates in antiphase relation with respect to the free-surface elevation, with amplitudes of almost 20 m. The presence of the submarine Algeciras Canyon was found to be determinant in the three-dimensional structure of tidal currents within the Bay, strengthening the baroclinic tidal regime of currents. This situation has quantitative consequences for the flow-exchange processes between Algeciras Bay and the outer Strait, with rates 20 times higher than those obtained when considering only the barotropic behavior, as well as inflow/outflow lateral recirculation volumes during half a tidal cycle that account for more than 20% of the net accumulated volume. This flow-exchange system was found to be affected by the nonlinear interaction processes between the first baroclinic period of resonance of Algeciras Bay and the M_2 tide.

Citation: González, C. J., Ó. Álvarez, R. Mañanes, A. Izquierdo, M. Bruno, J. J. Gomiz, J. Chioua, and L. López (2013), Baroclinic M_2 tidal circulation in Algeciras Bay and its implications for the water exchange with the Strait of Gibraltar: Observational and 3-D model results, *J. Geophys. Res. Oceans*, *118*, 5398–5411, doi:10.1002/jgrc.20404.

1. Introduction

[2] The displacement of the isopycnal surfaces around the pycnocline and changes in the vertical structure of tidal currents are two of the physical manifestations of tidal phenomena in stratified domains. This paper analyzes the M_2 tidal circulation in Algeciras Bay, and highlights the differences from the vertical structure dominant in the adjacent Strait of Gibraltar. The well-known hydrodynamic system of the Strait of Gibraltar is determined mainly by a mesotidal, semidiurnal regime, in conjunction with a strongly stratified water column due to the flow exchange between Atlantic and Mediterranean waters [see, e.g., *Candela et al*., 1990; *Mañanes et al*., 1998]. Other important contributions are made by subinertial processes related to the meteorology [*Lacombe and Richez*, 1982; *Candela et al*., 1989; *Dorman et al*., 1995; *Vázquez et al*., 2008]. The tidal dynamics of the Strait of Gibraltar has also been studied extensively. The most remarkable characteristic is the small variability of the vertical profiles of tidal currents, particularly those related to the dominant M_2 constituent. This behavior is shown by field data from current profilers throughout the water column [*Bruno et al*., 2000; *Tsimplis*, 2000], and explains the good agreement between barotropic, depth-averaged models of the Strait [e.g., *Tejedor et al*., 1998, 1999] and three-dimensional models [*Sannino et al*., 2007]. For the principal astronomical tidal constituents, the barotropic mode accounts for more than 90% of total variance of tidal currents over the Camarinal Sill [*Candela et al*., 1989; *Bruno et al*., 2000; *Sánchez-Román et al*., 2008] and about 70% in the eastern side of the Strait [*García-Lafuente et al*., 2000]. However, in particular areas of the Strait of Gibraltar, such as Algeciras Bay, this may

[1]Department of Applied Physics, University of Cadiz, Puerto Real, Cadiz, Spain.
[2]Centre Régional de Tanger, Institut National de Recherche Halieutique, Tangier, Morocco.
[3]National Institute of Water and Atmospheric Research (NIWA), Lauder, Omakau, New Zealand.

Corresponding author: C. J. González, Department of Applied Physics, University of Cadiz, CASEM, Campus Universitario de Puerto Real, Puerto Real, ES-11510 Cádiz, Spain. (carlosjose.gonzalez@uca.es)

2169-9275/13/10.1002/jgrc.20404

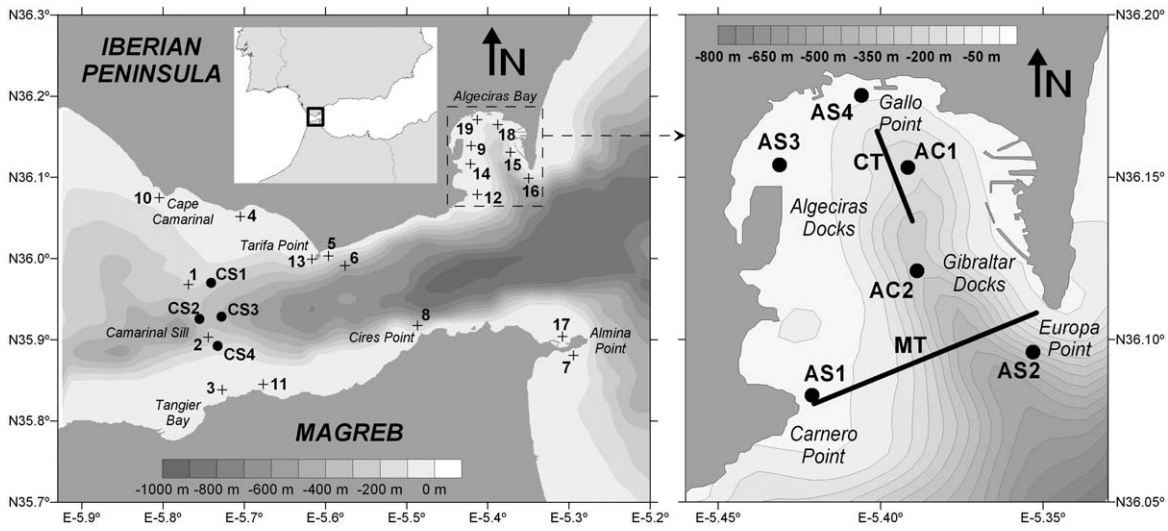

Figure 1. Geography and bathymetry of the Strait of Gibraltar: (left) coinciding with the domain of the model) and (right) a detail of Algeciras Bay. The figure also shows the stations for the model comparison of M_2 surface elevation (crosses: 1–19), and current velocity profiles (solid circles) at the Camarinal Sill (CS1–CS4), the shoreline of Algeciras Bay (AS1–AS4), and the Algeciras Canyon (AC1 and AC2, the latter also used as a control point for different analyses); also shown are the transects where the vm-ADCP measurements of currents were carried out (black lines) at the head of the canyon (CT) and the mouth of the Bay (MT).

be not the case. In this study, we try to verify if the general M_2 tidal dynamics of the Strait as a whole is also representative of this Bay.

[3] Algeciras Bay constitutes a semienclosed environment located at the northeastern limit of the Strait of Gibraltar (Figure 1), with particular economic importance due to high population density, intensive port activities, and coastal petrochemical industries. The depth of the Bay reaches 500 m near the mouth of the Algeciras Canyon, a submarine canyon that constitutes its longitudinal axis. Due to the wide and deep connection between Algeciras Bay and the Strait of Gibraltar, the hydrodynamic regime of the Bay is determined to a great degree by that of the Strait. This argument is supported by *Álvarez et al*. [2011] regarding the effects of incoming baroclinic internal wavefronts, generated in the Strait of Gibraltar over the Camarinal Sill, on the dynamics of Algeciras Bay. However, except for that study, the pioneer work by *De Buen* [1924], the preliminary information published in the *Environmental Quality Plan for the Campo de Gibraltar Dossier* [2004], and the recent work by *Chioua et al*. [2013], there are notably few studies of this topic. In particular, no specific studies have been conducted to date on the detailed characteristics of the M_2 tidal circulation in Algeciras Bay, nor its connection with the larger system constituted by the Strait of Gibraltar.

[4] In this paper, the M_2 tidal circulation in Algeciras Bay is described and discussed, with special emphasis on its vertical structure and the impact on the flow-exchange processes between the Bay and the Strait of Gibraltar. The effect of the Algeciras Canyon on the field of M_2 tidal currents within the Bay is analyzed as well. We use hydrodynamic modeling and a broad set of field data from tidal gauges, current meters, acoustic Doppler current profilers (ADCP), and salinity CTD sensors. Since the main focus of this study is the analysis of the tidal circulation related to the M_2 constituent, the spring and neap tidal cycles (resulting from the combination of the M_2 and S_2 constituents) are not considered. However, the behavior of the S_2 tidal dynamics in the Strait of Gibraltar was found to be analogous to that of the M_2 by *Tejedor et al*. [1999], so the results presented here could constitute a first approach for the study of the S_2 characteristics as well. The paper is organized as follows: section 2 presents the main characteristics of the three-dimensional model and the numerical simulation. The experimental data set used in this study is described in section 3. The predicted M_2 tidal circulation is presented and compared with observational data in section 4. Section 5 gives a detailed description of the vertical structure of M_2 tidal currents within Algeciras Bay, emphasizing differences with respect to that of the outer Strait of Gibraltar, as well as the influence of the Algeciras Canyon. In section 6, we show the impact that the three-dimensional structure of currents may have on the water-exchange flows between the Bay and the Strait. Finally, a discussion on the main results is presented.

2. The 3-D Model

[5] The three dimensional, nonlinear, high resolution, baroclinic, hydrodynamic UCA 3-D model [*Álvarez et al*., 2011] solves numerically the 3-D primitive equations in sigma coordinates, as described by *Mellor* [1996]. The vertical viscosity and diffusion are parameterized by a *Mellor and Yamada* [1982] second-order closure scheme. The model splits the 2-D (depth-averaged) equations coupled to the 3-D schemes. The solution of the 2-D equations provides the free-surface elevation and the mean depth-averaged velocity profiles. In correspondence, the 2-D

terms of advection, horizontal and vertical diffusivity, and baroclinic pressure gradient are calculated by the three-dimensional equations by integrating over the depth, while the bottom stress is solved by matching the numerical solution to the "law of the wall" near the bottom, setting a standard drag coefficient $C_D = 0.003$. The equations are integrated on an Arakawa-C staggered grid using a semiimplicit Crank-Nicolson scheme for the horizontal structure equations, while an implicit scheme is used for the vertical diffusion terms in the 3-D equations [*Richtmyer and Morton*, 1967].

[6] The grid domain includes the Strait of Gibraltar and the western zone of the Alboran Sea (see Figure 1, left), with a horizontal resolution of 100 m and 50 sigma levels in the vertical. The bathymetry, shown in Figure 1, was obtained from the Spanish Navy Hydrographic Institute (IHM) nautical charts. A radiation condition, written in terms of the deviations of tidal elevation and velocity from their observed values, was employed at the open boundaries to ensure the propagation of disturbances away from the model domain. The model was forced at the western and eastern open boundaries with a M_2 tidal wave, in terms of amplitudes and phases of free-surface elevation and velocity of currents, inferred from the previous studies by *Tejedor et al*. [1998], *Bruno et al*. [2000], *Tsimplis* [2000], and *Izquierdo et al*. [2001], using interpolation/extrapolation techniques and basic flow-conservation laws. Similarly, a steady baroclinic exchange was imposed at the boundaries, based on constant mean Atlantic and Mediterranean flows of 1.19 Sv (East directed) and 1.14 Sv (West directed), respectively, as inferred from the description given by *García-Lafuente et al*. [2002]. The seasonal variability of this steady exchange was not taken into account since it is beyond the scope of this study, which only focuses on the M_2 tidal dynamics.

[7] The initial spatial distribution of salinity and temperature was prescribed as a horizontally homogeneous field, according to field data collected during the Experiment "Strait 94–96" and the results given by *Bray et al*. [1995], *Bruno et al*. [2000], and *Izquierdo et al*. [2001]. They show that the general pattern of the Strait is constituted by two density-defined water layers (the upper Atlantic and the lower Mediterranean), and a zone of transition between the layers at depths ranging from 50 to 200 m. In the model experiment, the initial depth of the interface between the two layers was ~80 m, defined as the 37.5 isohaline according to *Candela et al*. [1989] and *Bruno et al*. [2002]. At the open boundaries, the salinity and temperature conditions are prescribed by means of a standard upstream advection scheme.

[8] The equations of motion were supplemented with smoothing terms, defined by a horizontal eddy diffusion operator acting throughout the model domain. The horizontal eddy viscosity coefficient was chosen to be as small as possible and, at the same time, capable of suppressing short wavelength disturbances in the field of tidal characteristics. These requirements were achieved by $K_0 = 0.05\ m^2\ s^{-1}$. The time step for integration was 2 s, which ensures the stability of the numerical solution.

[9] Output series from the last 10 M_2 cycles, once a steady time-periodic solution was achieved, were processed by techniques of harmonic analysis [*Foreman and Henry*, 1989] to obtain the M_2 tidal characteristics for the free-surface elevation, the 3-D tidal current field, and the interface between the upper Atlantic and the lower Mediterranean water layers. Additional details about the model and numerical experiment can be found in *Álvarez et al*. [2011].

3. Experimental Data

3.1. Tidal Elevation

[10] The amplitudes and phases of the M_2 tidal elevation at 19 experimental stations of the Strait of Gibraltar and Algeciras Bay were taken from the works by *García-Lafuente* [1986], *Candela* [1990], *Tsimplis et al*. [1995], the NOAA *World Ocean Circulation Experiment* [1990–2002], *García* [2006], *Pairaud et al*. [2008], and *Álvarez et al*. [2011] (locations 1–19 in Figure 1).

3.2. Tidal Currents

[11] The characteristics of the M_2 tidal currents within the study site were obtained from both available information and new data recordings. The vertical profiles of the M_2 current ellipse parameters over the Camarinal Sill published by *Candela* [1990], *Bruno et al*. [2000], and *Tsimplis* [2000] were used to describe the main characteristics of the M_2 tidal currents in the Strait of Gibraltar (CS1–CS4 in Figure 1). At the four stations located in nearshore areas of Algeciras Bay, the profiles of the ellipse parameters were obtained from the harmonic analysis of a 2 month experimental current series recorded during November to December 2006 by three ADCPs installed at a depth of ~20 m (AS1, AS3, and AS4), and two current meters moored at depths of 20 and 180 m (AS2). Analog analyses were made of the 3 month series recorded during November 2011 to January 2012 by two moored ADCPs along the Algeciras Canyon (AC1 at a depth of ~200 m, and AC2 at a depth of ~350 m) with a vertical resolution of 4 m. The vertical current profiles were supplemented by the current velocity at different tidal stages in two transects measured by a vessel-mounted ADCP (vm-ADCP): a longitudinal transect through the upper region of the Algeciras Canyon on 7 December 2006 (CT), and a transversal transect through the mouth of Algeciras Bay on 2 December 2006 (MT), both close to the spring phase of the tide.

3.3. Water Salinity

[12] To obtain the stratification profile of the water column in Algeciras Bay, three CTDs at depths of 40, 100, and 175 m provided salinity, temperature, and pressure during 23 days in November 2006 with a sampling interval of 1 min, at the AC2 station over the Algeciras Canyon. Complementing these observations, the mean salinity profile at the same location was obtained by time-averaging CTD hourly casts during one M_2 tidal cycle, on 11 November 2006 at the end of the neap phase of the tide.

4. Experimental Comparison of the Predicted M_2 Tidal Characteristics

4.1. M_2 Tidal Elevation

[13] Model results for the characteristics of the M_2 tidal elevation are presented in Figure 2, where the differences

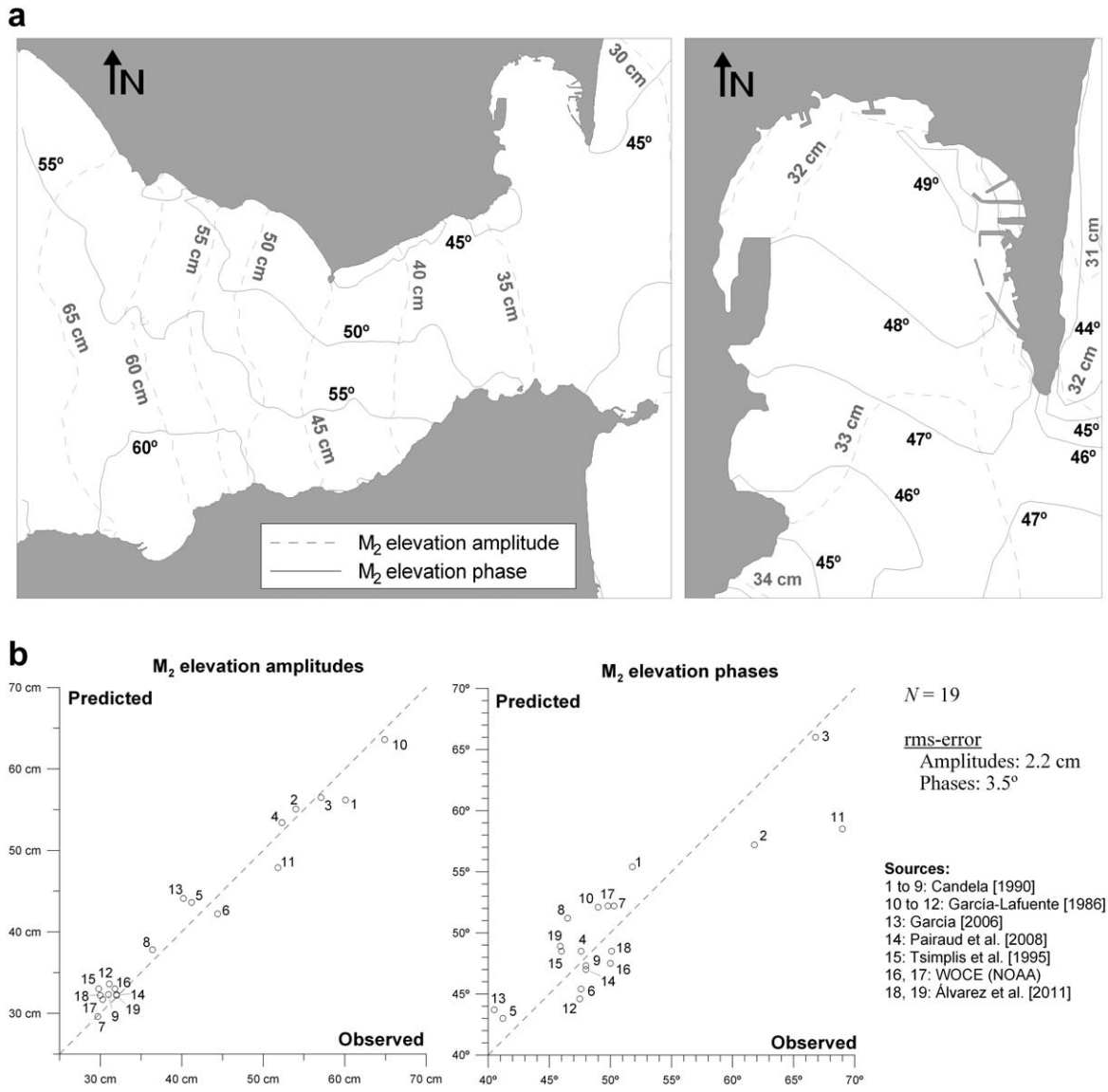

Figure 2. (a) Tidal charts for the M_2 elevation (solid lines: cotidal, in Greenwich degrees; dashed lines: corange, in cm), for (left) the Strait of Gibraltar and (right) a detail for Algeciras Bay. (b) Comparison between predicted and observed data for the (left) M_2 amplitude and (right) phase; the numbers correspond to the locations of experimental stations shown in Figure 1 (left).

between the model predictions and observational data for the entire domain are also shown. The predicted M_2 amplitude field (Figure 2a) shows a smooth variation along the Strait, decreasing from 65 cm at the western limit to 30 cm at the eastern boundary. Phases, in accordance with *Candela* [1990], *Tejedor et al*. [1998], and *Sannino et al*. [2007], show small variations close to 15°, giving evidence of slight wave propagation south westwards. In Algeciras Bay, the amplitude of the M_2 tide remains around 33 cm and the cotidal lines indicate a northward propagation, as well as M_2 wave diffraction around the headland constituted by the Rock of Gibraltar. Within the Bay, the Greenwich tidal phase ranges from 46° at the mouth to 49° at the northeastern head.

[14] The comparison between the predicted and observational M_2 tidal characteristics is shown in Figure 2b for 19 stations. The values of the root-mean-square (RMS) errors for the harmonic parameters from all the stations shown in Figure 1 (left) (2.2 cm for the amplitudes and 3.5° for the phases), small when compared with the ranges of spatial change within the Strait of Gibraltar, show that the model results are representative of the M_2 tidal hydrodynamics in this environment.

4.2. M_2 Tidal Currents

[15] Figure 3 shows the comparison of model results with the vertical profiles of M_2 current ellipse's parameters recorded in eight locations, four over the Camarinal Sill (CS1–CS4), and four close to the shoreline of Algeciras Bay (AS1–AS4). Over the Camarinal Sill (Figure 3a), the vertical profiles of the M_2 current ellipse parameters reveal a predominant barotropic pattern. Here, for every station,

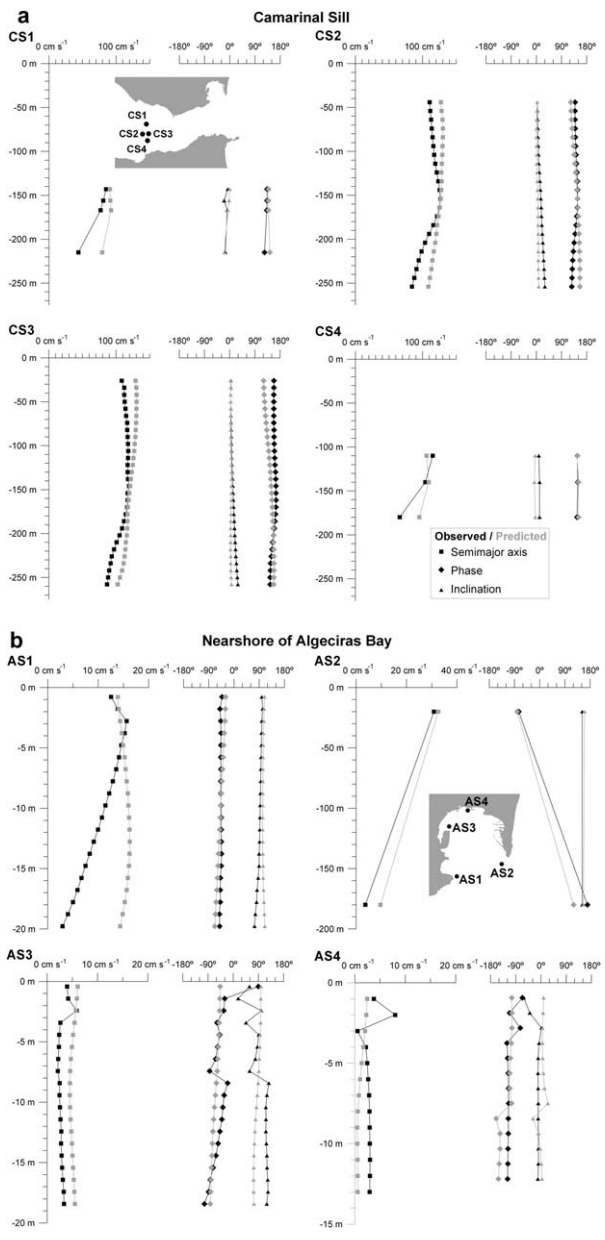

Figure 3. Observed (black) and predicted (gray) vertical profiles of the M_2 current ellipse parameters: (a) stations over the Camarinal Sill; CS1, CS4: *Candela* [1990]; CS2: *Bruno et al*. [2000]; CS3: *Tsimplis* [2000] and (b) stations in the nearshore areas of Algeciras Bay; AS1–AS4. Squares: semimajor axis; diamonds: ellipse phase (in Greenwich degrees); triangles: ellipse inclination (0° eastwards, positive anticlockwise).

both observed and predicted amplitudes and phases of currents present small vertical variations. The agreement between observed and predicted M_2 ellipses is shown by the RMS errors for the semimajor axes (14 cm s^{-1}) and phases (12°). At the four near-shore stations in Algeciras Bay (Figure 3b), the RMS errors are 4.4 cm s^{-1} for the M_2 semimajor axes and 15.9° for the phases. The relatively high RMS errors at the AS1 and AS4 stations could be related to: (a) local-scale bathymetric features not considered by the model, which would imply differences in the effect of bottom friction and (b) the low correlation coefficients (50% ± 20%) of the harmonic analysis of observed currents at different depths at these locations, due to the weakness of tidal currents and the complexity related to other possible forcing mechanisms. However, these data require further comments. Note that, in the shallow AS1, AS3, and AS4 stations, the characteristics of the M_2 tidal currents show greater vertical homogeneity than at the deeper AS2 station, where the M_2 tidal currents reach 30 cm s^{-1} at 20 m depth, and slow down to 10 cm s^{-1} at a depth of 180 m, while the phase-lag between the two depths is close to 180°, as also reproduced by the numerical model. Since AS1, AS3, and AS4 locations only monitor the upper 20 m layer of water, additional data and analyses are necessary to explain the complete vertical structure of the M_2 tidal currents in the whole deeper area of Algeciras Bay.

[16] Figure 4 shows the vertical profiles of current ellipse parameters at two stations over the Algeciras Canyon, one in the northern region close to the head of the Canyon (AC1) and the other further south over the Canyon (AC2). The corresponding results from the modeling experiment are also shown for comparison. Despite the quantitative differences between observed and predicted profiles (RMS errors of 4.3 cm s^{-1} for semimajor axes and 32.4° for

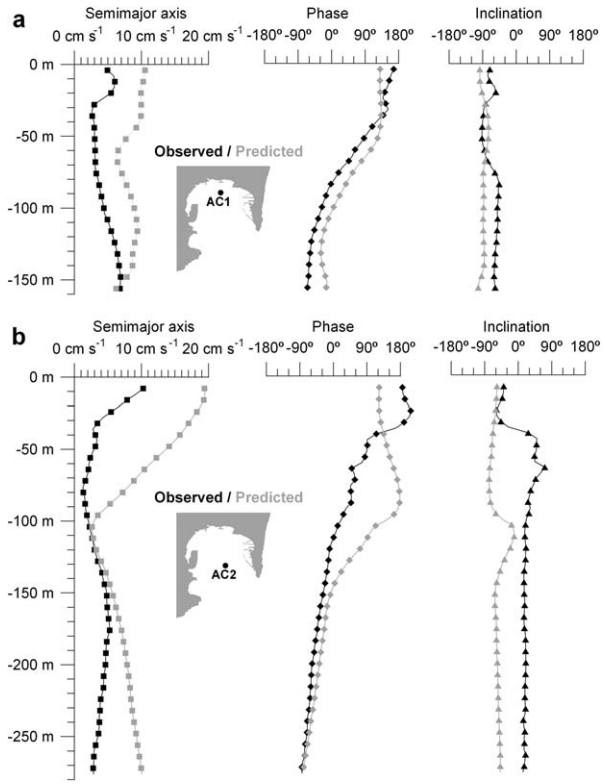

Figure 4. Observed (black lines) and predicted (gray lines) vertical profiles of the M_2 current ellipse parameters over the Algeciras Canyon: (a) station AC1 at the northern head of the canyon and (b) station AC2 further south over the lower canyon. Squares: semimajor axis; diamonds: ellipse phase (in Greenwich degrees); triangles: ellipse inclination (0° eastwards, positive anticlockwise). Symbols are plotted every 2 ADCP cells.

phases at AC1, and 6.4 cm s^{-1} and 64.0° at AC2), the model seems to be capable of reproducing the observed near 180° phase shift with depth. At AC2, the model overestimates the current amplitudes by ~6 cm s^{-1} on average, and the observed inclinations of ellipses are almost orthogonal to their predicted values. Differences in ellipse inclination and semimajor axis at AC1 and AC2 are attributable to local-scale topographic features unresolved by the model bathymetry, which are more determinant over the mouth of the Canyon due to the reduction of the flow characteristic length scale [see, e.g., *García-Lafuente et al*., 1999; *Allen and de Madron*, 2009], as will be further discussed.

5. Vertical Structure of M_2 Currents in Algeciras Bay

[17] As can be seen in Figure 4, two relative maxima for the current amplitudes are observed, one in the upper Atlantic and the other in the lower Mediterranean water layer, with a near-zero minimum at the interface. Correspondingly, there is a phase-lag of nearly 180° between the two layers, indicating the existence of a counter-current tidal system within the Bay. The tidal counter-current system becomes more evident in Figure 5, which shows a time sequence of current velocity in the ebb/flood direction (flood positive), defined with an inclination of 25° (anticlockwise) with respect to the North direction, in a longitudinal transect running along the head of the Algeciras Canyon. Currents measured by the vm-ADCP (Figure 5, left) are plotted together with the corresponding results from the numerical experiment for the same tidal stages (Figure 5, right). The most striking feature seen in both observed and predicted data is the presence of the mentioned tidal counter-current system between the upper Atlantic and the lower Mediterranean water layers, so the maximum water inflow in one layer is close in time to the maximum outflow in the other layer, the velocity decaying to zero close to the interface between the two layers, at a depth of about 50–100 m. The quantitative and qualitative discrepancies between observed and modeled results (i.e., the phase differences present in some of the panels and the higher observed currents) are related to the effect of constituents other than the M_2 during the measurements, since they were made close to the spring phase of the tide [see *Chioua et al*., 2013].

[18] Completing the description of this current system, we also studied the predicted depth-averaged velocity field through each water layer (Atlantic and Mediterranean), characterizing the separating interface as the 37.5 isohaline (except in those shallow areas with no Mediterranean layer, where the bottom depth was taken as the lower limit). The two-layer salinity structure is confirmed at the AC2 station as shown in Figure 6a, where three CTD sensors at different depths show clear tidal oscillations, with values ranging from 36.5 to 37.2 at 40 m depth, from 37.2 to 38.0 at 100 m depth, and from 38.0 to 38.4 at 175 m depth, which are reproduced by the M_2 model simulation with maximum RMS errors of ~0.2 practical salinity units. This agreement is more evident in the mean salinity profile (time averaged over one M_2 cycle) at the same point. As can be seen in Figure 6b, small differences with respect to model results are obtained, taking into account the range of vertical variability involved.

[19] Now we can return to analyze the results for the predicted layer-averaged velocity field. Figure 7 shows the spatial fields of the predicted M_2 characteristics of the interface depth and the depth-averaged currents of both layers, in terms of their amplitudes and phase differences (leads) with respect to the free-surface elevation. As shown in Figure 7a, the M_2 amplitude of the interface depth oscillations increases toward the head of Algeciras Bay, from about 9 m at the mouth of the Bay to more than 20 m near the northern coast, while the phase reaches almost antiphase values with respect to the tidal elevation within the inner Bay. Correspondingly, the M_2 depth-averaged currents in the Atlantic (Figure 7b) and the Mediterranean (Figure 7c) layers have an opposing time pattern, the Atlantic and Mediterranean currents being in quadrature relationship with the tidal elevation and the interface depth, respectively. Hence, as the free-surface rises, the net flooding of the Bay is due to the inflow of upper Atlantic waters, which coincides with a simultaneous outflow of lower Mediterranean waters (mainly along the Algeciras Canyon), and consequently the thickness of the Atlantic layer increases and the interface is situated at a greater depth. Half an M_2 tidal cycle later, the situation will be the opposite. Observations (Figure 5) and model results (Figure 7) show that the Canyon is efficient in intensifying and directing bottom tidal currents to the head of the Bay, as reported by *Boyer et al*. [2000] and *Kämpf* [2007].

[20] In addition to these characteristics, other particular features can be seen in the behavior of the structure of currents in Algeciras Bay. Considering Figure 7b once again, a weakening in the amplitudes of currents in the Atlantic layer is observed in the deeper areas over the Algeciras Canyon. This is accompanied by strong lateral gradients of phase toward the coastal margins, with spatial differences of almost 30°: although in deeper regions the differences of phase between tidal elevation and currents are close to 90°, in shallower areas the differences reach 120°. These differences in amplitudes and phases are related to the fact that maximum tidal currents in the Atlantic layer are closer to the surface. This is explained by the weakening of currents near the interface depth, due to the increase of shear dissipation related to the counter-current system already described. Therefore, lower velocities and greater phase-lags are obtained when depth averaging in deeper places, where counter-current system is well developed, i.e., over the Algeciras Canyon.

[21] Continuing with the explanation of peculiarities in the M_2 tidal characteristics, a notable increase of the amplitude of M_2 tidal currents is detected in areas near the headland at the Rock of Gibraltar. In general, the presence of headlands influences the spatial structure of currents, forcing them to follow the coastal contours and increasing tidal currents due to volume conservation processes and irrotational flow trajectories around the headland. This interpretation is supported both by experimental data [*Pingree and Maddock*, 1979] and numerical models [*Tee*, 1976; *Signell and Geyer*, 1991]. In Algeciras Bay, the effect of the Rock of Gibraltar is no exception: irrotational flows around the headland are present in both layers, as well as an intensification of currents, reaching 30 cm s^{-1}.

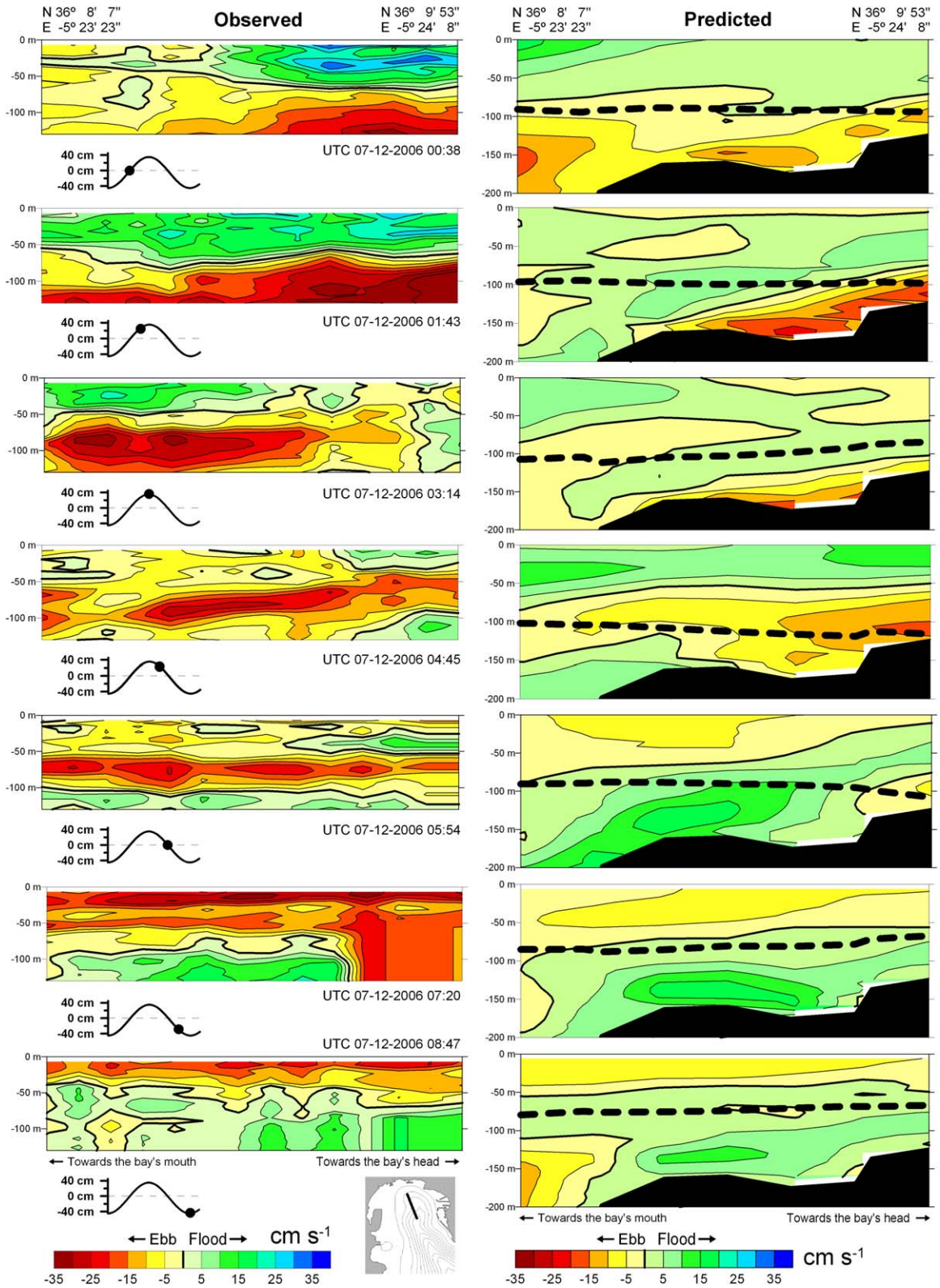

Figure 5. vm-ADCP measurements (left; data collected in a situation of near-spring tide, with tidal amplitudes of about 40 cm) and model results (right) for the velocity of currents in the ebb/flood direction (flood positive) along a longitudinal transect at the head of the Algeciras Canyon, for seven different tidal stages (from upper to lower, specified by the tidal elevation series below the observed transects). Thick black contour line: zero value (null current); thick black dashed line in predicted transects: interface depth (37.5 isohaline).

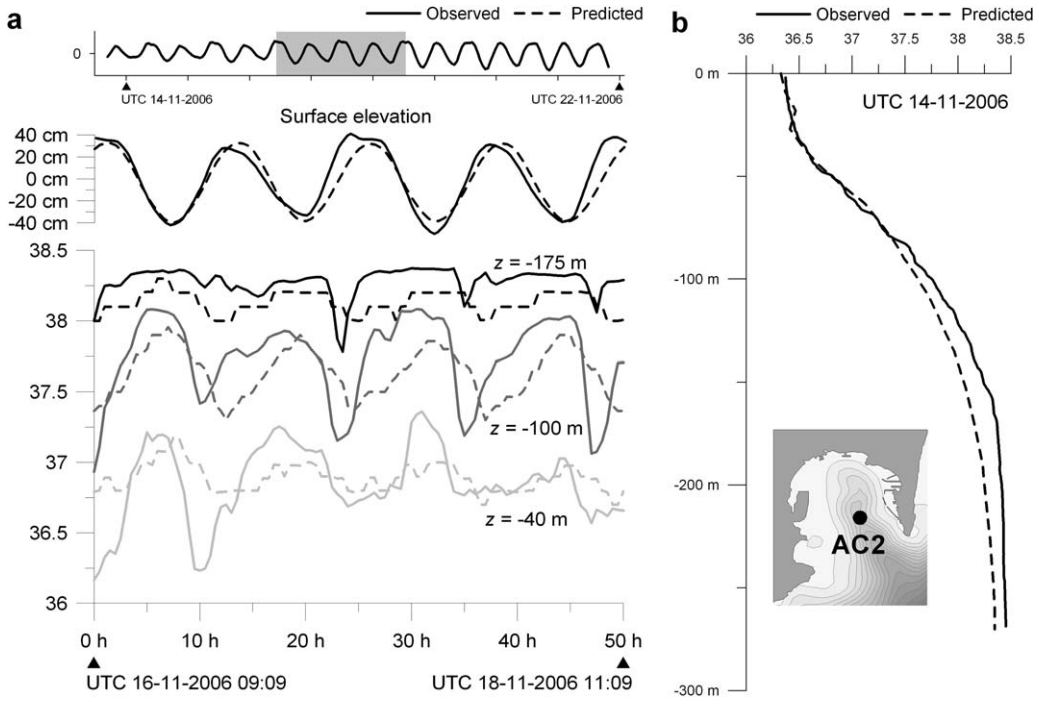

Figure 6. Comparison between observed (solid lines) and predicted (dashed lines) salinity structure of the water column at the control point AC2 over the Algeciras Canyon: (a) CTD-mooring salinity series during 4 M_2 tidal cycles in a mean-tide situation (shaded area in the top plot) at depths of 40 m (light gray line), 100 m (dark gray line), and 175 m (black line), together with the free-surface elevation series (top), and (b) mean CTD salinity profiles (averaged over one M_2 tidal cycle).

[22] In areas of Algeciras Bay that adjoin the Strait, different interacting patterns are visible. First, the dominant along-Strait tidal currents adjacent to the mouth of the Bay acquire a clearly observable across-Strait component, shown by an increase in the semiminor axes of tidal current ellipses, and hence decreasing their eccentricity. This is caused by the tendency of the Canyon to increase the ageostrophy of along-Strait tidal currents, evidenced by the appearance of an across-isobath velocity component. This effect of ageostrophy on tidal current ellipses has been reported by *Quaresma and Pichon* [2013] for different locations in the Iberian shelf. Second, within Algeciras Bay the tidal currents tend to follow the isobath contours, shown by the orientation of the semimajor axes parallel to the coastline. The resulting system is analogous to that described from field data by *Hickey* [1995], as well as laboratory and numerical model results by *Boyer et al*. [2004], *Haidvogel* [2005], and *Boyer et al*. [2006].

[23] Despite these peculiarities, results show a notable indication of a baroclinic standing wave pattern for the first internal tide mode, which is reported for other stratified bays and submarine canyons [*Lee et al*., 2009]. The baroclinic solution for the linear equations of momentum and continuity for a one-dimensional, two-layer, frictionless flow gives a rough estimation of the magnitude ratios and phase-lags between the upper limit displacement and depth-averaged currents of the two layers as $\xi_1/\xi_2 \simeq -g'h_2/[g(h_1+h_2)]$ and $u_1/u_2 \simeq -h_2/h_1$ [see, e.g., *Gill*, 1982], where h_i, ξ_i, and u_i are, respectively, the mean thickness, upper limit displacement, and depth-averaged current for the upper ($i=1$) and lower ($i=2$) layers (so ξ_1 is the free-surface elevation, and ξ_2 the displacement of the interface over its mean depth $-h_1$); g is the acceleration due to gravity; and $g' = g(\rho_2-\rho_1)/\rho_2$ is the reduced gravity, ρ_i being the water densities. This behavior, reproduced qualitatively by the numerical model results, characterizes the antiphase relationship of currents between layers and surface displacements by hydrostatic effects, indicated by the opposite signs of both sides of these expressions. Quantitatively, they imply interface displacements two to three orders of magnitude higher than those for free-surface elevation in Algeciras Bay, in accordance with the amplitudes of ξ_1 ($\sim$30 cm) and ξ_2 ($\sim$20 m) predicted by the model.

[24] The different nature of the M_2 tidal circulation in Algeciras Bay with respect to the Strait of Gibraltar is also highlighted by the Empirical Orthogonal Functions (EOF) analysis of the predicted M_2 currents at the control point AC2 within the Bay (Figure 8) and the comparison with the corresponding results for the Strait, over the representative Camarinal Sill location CS2. Although a direct identification of the EOF modes with the barotropic and baroclinic components of currents is not possible from this single analysis, differences between these two environments are evident. At the CS2 station, the first EOF mode, with high vertical homogeneity (and plausibly corresponding to the barotropic content according to *Bruno et al*. [2000]), represents more than 90% of the total variance of M_2 currents. In contrast, at the control point in Algeciras Bay the situation is more complex: the first and third EOF modes, with changes in sign through the water column (and hence plausibly related to the baroclinic content) explain together about 75% of the total variance of M_2 currents.

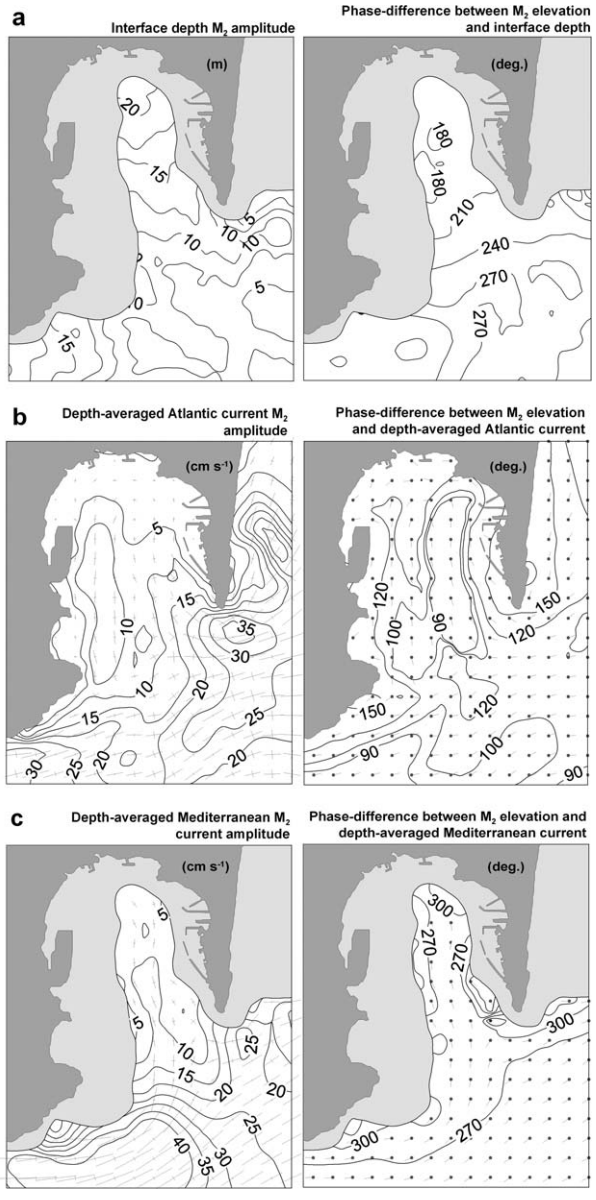

Figure 7. Predicted M_2 harmonic parameters for the two-layer system in Algeciras Bay: (a) amplitudes (left) and phase difference with respect to the free-surface elevation (right) for the interface depth, (b) current ellipse axes (left) and phase difference with respect to the free-surface elevation (right; symbols denote the direction of the ellipses: dots are phase origins, chosen to contemplate a flood situation in Algeciras Bay) for the tidal currents, depth-averaged over the upper Atlantic water layer, and (c) the same as in Figure 7b but for the lower Mediterranean water layer.

6. Implications for the Water-Exchange Processes

[25] The structure described above is the first step toward analyzing the water-exchange processes between the Algeciras Bay system and the outer Strait of Gibraltar. To this end, Figure 9 shows a time sequence of current velocity in the ebb/flood direction (defined as in Figure 5; flood positive) in a transversal transect through the mouth of Algeciras Bay, measured by a vm-ADCP (Figure 9, left), together with the corresponding results from the numerical experiment for the same tidal stages (Figure 9, right). Qualitative and quantitative differences between observed and predicted currents are mainly due to the near spring-tide phase during the experimental data acquisition, as previously commented. A mere visual inspection of Figure 9 reveals the two-layer dynamics in the mouth of the Bay to have a clear across-Bay structure, with simultaneous inflow/outflow occurrences within each layer. This structure is more evident in episodes close to the inversion of currents direction and is mainly related to the previously described lateral phase gradients and the along-Strait tidal currents from the Strait of Gibraltar.

[26] The water exchange between Algeciras Bay and the Strait of Gibraltar can be estimated from the complete sections at the mouth provided by the model. For each layer i (where $i = 1$ for the Atlantic layer and $i = 2$ for the Mediterranean layer as previously stated), the instantaneous net flow Q_i is defined by

$$Q_i = \int_{S_i} u_\perp dS_i \tag{1}$$

where $u_\perp(x, y, z, t)$ is the component of current velocity normal to the cross-section surface S_i at the mouth of the Bay (the interface depth being the limit between S_1 and S_2), chosen for the inflow to be positive. Due to the three dimensionality of the structure of currents (which may imply simultaneous inflow and outflow at different places within each layer), the layer net flow will be the sum of the inflow Q_i^+ and the outflow Q_i^- $\left(Q_i = Q_i^+ + Q_i^-\right)$, which are calculated as:

$$Q_i^+ = \int_{S_i} u_\perp dS_i \;;\; \forall u_\perp > 0 \tag{2}$$

$$Q_i^- = \int_{S_i} u_\perp dS_i \;;\; \forall u_\perp < 0 \tag{3}$$

[27] In Figure 10, the predicted time series of Q_i, Q_i^+, and Q_i^- are plotted during one M_2 tidal cycle. Hence, the blue/red-colored curves account for the recirculation processes for each layer (simultaneous inflow and outflow), while the net volume changes inside the Bay are only due to the Q_1 and Q_2 flows (black curves). As a reference, the series of free-surface elevation and interface depth, both spatially averaged throughout the Bay's area, are also shown, identifying the tidal stages represented in Figure 9. The situation shown by Figure 10 is analogous to the previously reported results from the spatial fields: a remarkable and necessary symmetry between the Atlantic and Mediterranean flows is clear, and the resulting instantaneous total net flow $Q = Q_1 + Q_2$ (not plotted) is one order of magnitude less than Q_1 and Q_2: the maximum total flow Q is 3.2×10^{-3} Sv compared with 8.6×10^{-2} Sv of Q_1 and 8.3×10^{-2} Sv of Q_2. The coincidence in time of the maximum Atlantic inflow (maximum Mediterranean outflow) with the

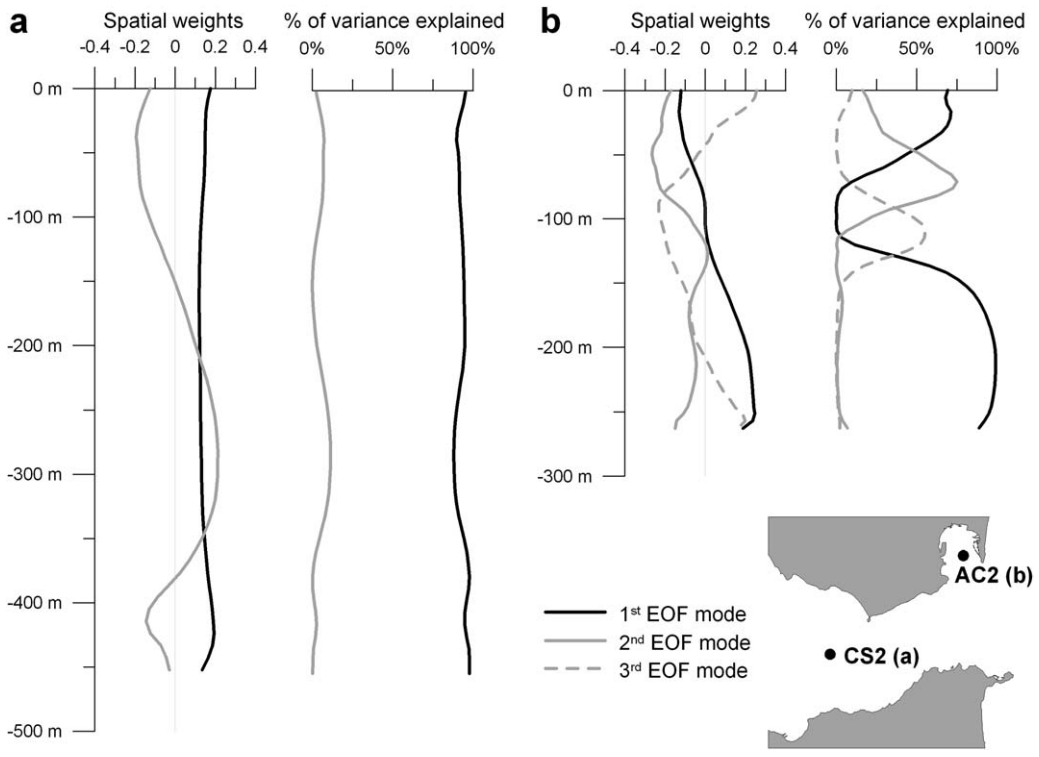

Figure 8. (a) First EOF modes together explaining more than 95% of total variance of the predicted ebb/flood tidal currents at the point CS2 over the Camarinal Sill and (b) the control point AC2 over the Algeciras Canyon, showing the spatial weights (left) and percentage of explained variance (right) for the first (solid black lines), second (solid gray lines), and third (dashed gray lines) EOF modes.

near-zero (rising) tidal elevation and mean (falling) interface depth (as well as the opposite situation half a M_2 period later) is explained by the antiphase relationship between the two layers, as described in the previous section.

[28] The inflow/outflow accumulated volumes of water in half a tidal cycle due to the calculated net flows are 754.0 Hm^3 for the Atlantic layer and 716.7 Hm^3 for the Mediterranean layer, which represent, respectively, 12% and 11% of the mean estimated total volume of Algeciras Bay ($\sim$6570 Hm^3). The recirculation flow in each layer can be calculated from the difference between the net flow and the inflow/outflow curves as $Q_i^r = \max\left(Q_i^+, |Q_i^-|\right) - |Q_i| = \min\left(Q_i^+, |Q_i^-|\right)$. The time integration of Q_i^r implies that the recirculation volume represents 20.0% of the net inflow/outflow accumulated volume during half a M_2 tidal cycle (i.e., a flooding/ebbing episode) in the Atlantic layer and 30.5% in the Mediterranean layer. These results emphasize that the lateral phase gradients and ageostrophy at the mouth of Algeciras Bay affect the flow-exchange structure, although the net exchange processes are related to the two-layer baroclinic tidal dynamics, promoted by the presence of the Algeciras Canyon. Results also show the importance of the baroclinic pattern for the water-exchange processes between Algeciras Bay and the Strait of Gibraltar, and hence on the transport rates within the Bay, which are estimated to be 20 times higher when considering the baroclinic two-layer transport system.

[29] Regarding the time variability of water transport through the mouth of Algeciras Bay, Figure 10 reveals that it cannot be explained simply by the single contribution of the M_2 constituent. The nonlinear-induced dynamics in the Strait of Gibraltar, and that generated within Algeciras Bay as well, produce appreciable asymmetries. The harmonic analysis of the total flow time series in each layer supports this interpretation, showing that more than 99% of total time variability of flows is due to the contributions of the main M_2 constituent, its nonlinear harmonics M_4, M_6, and M_8, and the M_3 tidal harmonic. In the Atlantic layer, the flow amplitudes are 0.054 Sv for the M_2 constituent, with amplitude ratios of 0.09 for M_4/M_2, 0.18 for M_6/M_2, 0.24 for M_8/M_2, and 0.04 for M_3/M_2. Similar values are obtained for the Mediterranean layer, as expected from the volume conservation: 0.051 Sv for M_2, and ratios of 0.08 for M_4/M_2, 0.24 for M_6/M_2, 0.31 for M_8/M_2, and 0.04 for M_3/M_2. In this case, all constituents are nearly in antiphase with respect to those in the Atlantic layer.

[30] The higher flow amplitude of the M_8 constituent with respect to the M_4 and M_6 in both layers is notable. This may be explained as follows: the resonant period for the first baroclinic mode in Algeciras Bay can be estimated from a two-layer approximation as $T_r = 4L[g'h_1h_2/(h_1+h_2)]^{-1/2}$, where L is the length of Algeciras Bay (about 9 km where the two layers coexist). This expression provides a value for T_r of about 5.1 h, which is also supported by experimental data from the AC2 station. Figure 11 shows the spectrum of ADCP-measured horizontal currents at this location at a depth of 40 m, chosen because of the clearer nonlinear signal due to the weakening of the M_2 currents at this level. In order to obtain the highest resolution for frequencies, the

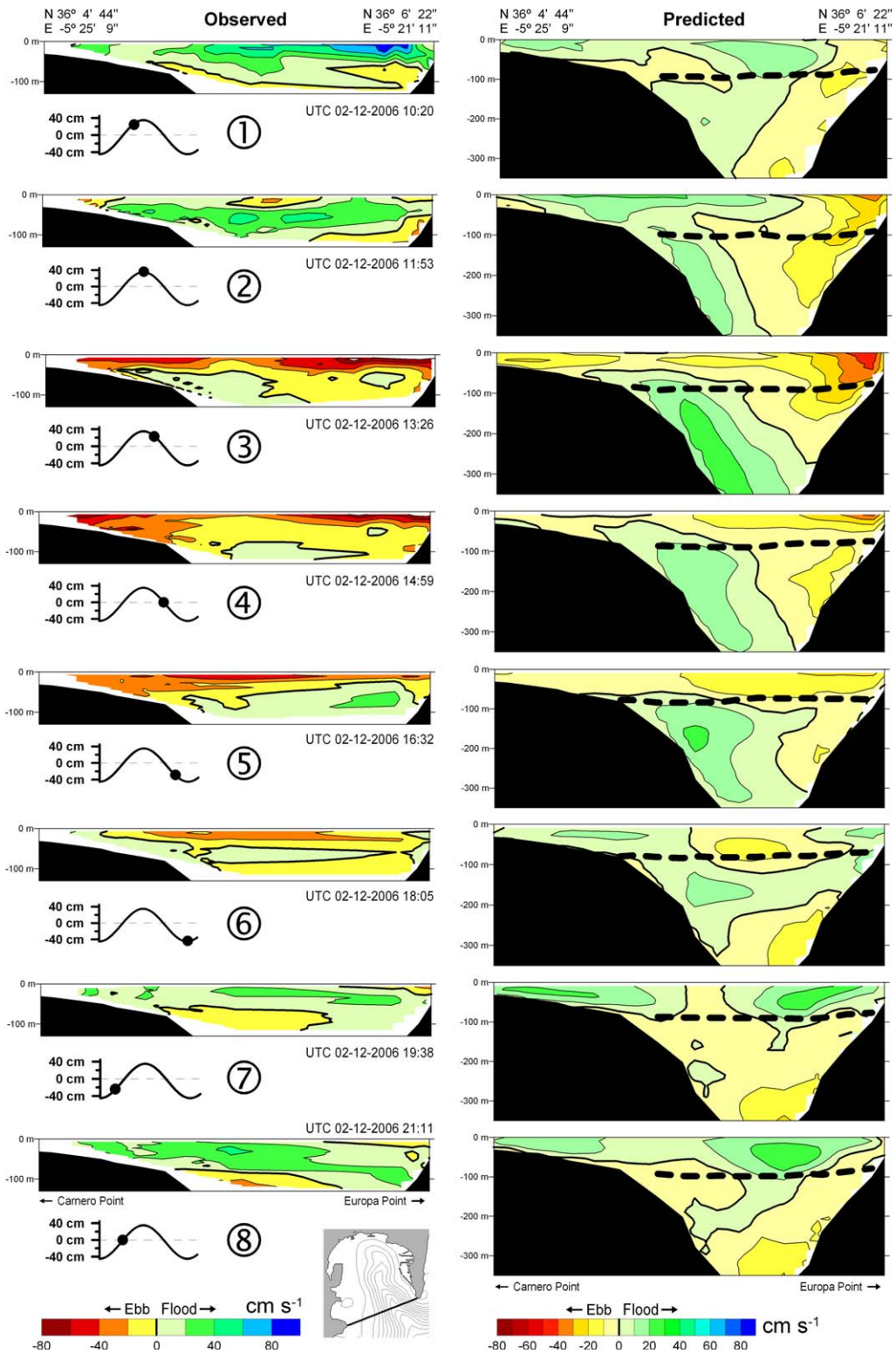

Figure 9. vm-ADCP measurements (left; data collected in a situation of near-spring tide, with tidal amplitudes of about 40 cm) and model results (right) for the velocity of currents in the ebb/flood direction (flood positive) along a transversal transect at the mouth of Algeciras Bay, for eight different tidal stages (from top to bottom, specified by the tidal elevation series below the observed transects). Thick black contour line: zero value (null current). Thick black dashed line in predicted transects: interface depth (37.5 isohaline).

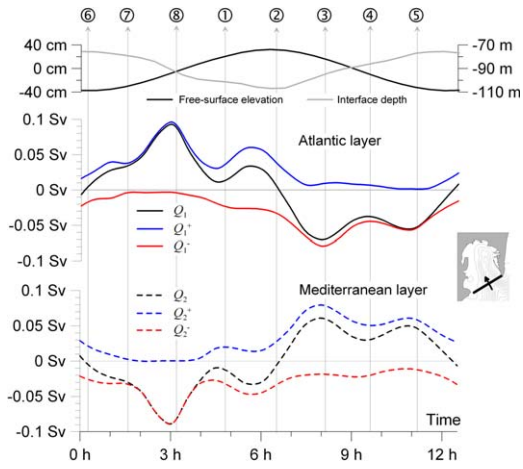

Figure 10. Predicted series of Atlantic (center, solid lines) and Mediterranean (down, dashed lines) water flows through the mouth of Algeciras Bay during one M_2 tidal cycle (black: net flows; blue: inflows; red: outflows; flood direction positive), together with the corresponding series (up) of surface elevation (black line, left vertical axis) and interface depth (gray line, right vertical axis), averaged over the area of the Bay. Tidal stages represented in Figure 9 are identified by numbers inside circles.

number of frequency bands was the maximum allowed by the Nyquist criterion, according to the length and sampling interval of the time series, so the frequency step between bands was $8.32 \cdot \times 10^{-7}$ s^{-1}. A clear peak of spectral density is present quite close to the estimated baroclinic resonant period of 5.1 h. To a greater or lesser degree, the same analysis of data from all ADCP cells gives similar results. Since the water flow gets a significant contribution from the nonlinear interaction between the current velocity and the M_2 oscillation of the interface depth (with a period $T_{M2} = 12.42$ h), there will be a signal intensification at the frequencies resulting from the resonant $(\omega_r = 2\pi/T_r)$ and M_2 $(\omega_{M2} = 2\pi/T_{M2})$ frequencies as $\omega_1 = \omega_r + \omega_{M2}$ and $\omega_2 = \omega_r - \omega_{M2}$. The period related to ω_1 is 3.6 h, which is quite close to the characteristic period of the M_8 constituent (3.11 h) and contributes to its relatively high flow amplitudes. In addition, the corresponding period for ω_2 is 8.6 h and could be related to the characteristic period of the M_3 constituent (8.28 h), which is also present in the results of the flow harmonic analysis, although having less relative amplitudes (4% of the M_2 flow) since its origin comes mainly from that nonlinear process. As was shown for the M_2 barotropic mode by *Álvarez et al*. [2011], the model seems to be able to reproduce the resonant characteristics of the baroclinic M_2 dynamics in Algeciras Bay as well.

[31] For each water layer, the time-integrated net flows during a complete M_2 tidal cycle are not significant, which implies the net water exchange between layers by net residual advective vertical transport to be insignificant as well. This situation is consistent with the weakening of net vertical transports in stable stratified domains [see, e.g., *Skliris et al*., 2007]. According to *Waterhouse et al*. [2009], a criterion for determining the strength of the advective regime in driving upwelling processes in canyons is the advective Rossby number. If it is greater than 0.2, there is a driving flow characterized by upwelling at the convergence of isobaths at the head of the canyon, and the flow in the upstream areas is not blocked. In contrast, such upwelling processes are not quantitatively significant in Algeciras Bay, due to the presence of coastal boundaries that prevent their development in the region where the isobaths converge at the head of the Canyon. Here, the calculated Rossby numbers are below 0.06 (compared with values of ∼0.3 present at the mouth of the Canyon) and net vertical currents are insignificant, in contrast with the net upwelling/downwelling processes observed in isolated canyons with no coastal blocking at the head [see, e.g., *Hickey*, 1997; *Boyer et al*., 2006]. However, the instantaneous vertical tidal currents reach values of 0.5 cm s^{-1} at some places within the northern-most part of the Algeciras Canyon, and the role of diffusive processes related to the internal waves field on the vertical transport may be significant, as established by *Chioua et al*. [2013] from field measurements.

7. Concluding Remarks

[32] In this paper, we have tried to gain insights into the M_2 tidal dynamics in Algeciras Bay and how these dynamics are related to those of the Strait of Gibraltar. The study has been conducted using a three dimensional, high resolution, baroclinic model, complemented, and supported by observational data. Results show that the barotropic characteristics predominant in the Strait of Gibraltar cannot be extrapolated into Algeciras Bay, where the effects of the water stratification on the tidal dynamics forced from the Strait generate current systems of clear baroclinic nature. While more than 80% of the M_2 tidal variance in the Strait of Gibraltar is barotropic and its dynamics is well represented by barotropic models, the situation in Algeciras Bay is determined by its baroclinic character. This conclusion is supported by EOF analysis, showing that at least 75% of the total variance of M_2 current velocity field in Algeciras Bay is plausibly related to baroclinic processes. The reasons for such a situation have to do with the semienclosed character of Algeciras Bay and the existence of a deep submarine canyon.

[33] The M_2 tidal currents in Algeciras Bay depend on the morphology of the Bay and on the water column stratification, as well as on the open boundary tidal forcing. This

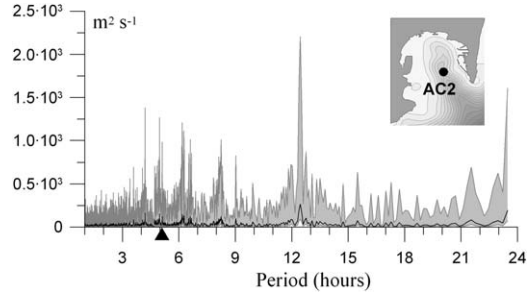

Figure 11. Spectral distribution of observed horizontal current (in terms of semimajor axes for each frequency band) at 40 m depth at the AC2 station, for periods between 1 and 24 h. The 95% confidence intervals are shaded in gray. The 5.1 h baroclinic resonant period of Algeciras Bay is indicated by a black triangle.

dependence, of course, is not exclusive to Algeciras Bay. In fact, its general behavior is quite well explained by the theory of two-layer tidal flow dynamics in stratified, semi-enclosed domains, and it has also been similarly described for other systems such as the Gareloch [*Elliot et al*., 2003], the Gaoping submarine canyon [*Lee et al*., 2009], and Liverpool Bay [*Palmer*, 2010]. However, the deep central canyon of Algeciras Bay strengthens the baroclinic tidal regime since it allows the full development of the vertical stratification structure in the water column. This results in the presence of strong lateral gradients of phases and amplitudes of Atlantic water tidal currents toward shallower areas. Although the tidal flow structure in Algeciras Bay is affected by this lateral variability, as well as the barotropic circulation from the Strait of Gibraltar, the net water exchange processes are mainly determined by the two-layer dynamics related to the strong baroclinic tide, promoted by the presence of the Algeciras Canyon. Results, therefore, imply a qualitative particular behavior of Algeciras Bay with respect to the predominantly barotropic regime of the Strait of Gibraltar.

[34] The present work focuses on the analysis of tidal currents in Algeciras Bay related to the constituent M_2 for representative stratification conditions. Other factors not considered in this study, as the spring/neap tide episodes and the seasonal variation of the water stratification structure, could imply certain deviations from the mean situation presented here, as shown by *Tsimplis* [2000] and *Vargas et al*. [2006] for the adjacent areas of the Strait, and these will be analyzed in future research. However, the numerical model has demonstrated its ability to reproduce the particular M_2 tidal dynamics in Algeciras Bay as a part of the general system constituted by the Strait of Gibraltar, supported by observational data. This structure of tidal counter-currents explains the high renewal rates existing in Algeciras Bay, in spite of the apparent weakness of the tidal influence when considering only the tidal range. These results also highlight the importance of coastal submarine canyons in cross shelf-break exchange, in accordance with *Hickey* [1995] and *Allen and de Madron* [2009]. The value of recognizing and understanding these processes in such a heavily populated, industrialized Bay with its harbors, ports, and dense maritime traffic, becomes evident.

[35] **Acknowledgments.** This study was partially supported by the Andalusian Government Project P06-RNM-01443; the Spanish Ministry of Education and Science Projects CTM2007-60408/MAR, CTM2008-06421/MAR, and CTM2010-20945/MAR; and the European Regional Development Fund (ERDF) in the framework of the ARCOPOLplus Project (Atlantic Area Transnational Programme). The authors thank the two anonymous reviewers for their valuable suggestions that have substantially improved this paper.

References

Allen, S. E., and X. D. de Madron (2009), A review of the role of submarine canyons in deep-ocean exchange with the shelf, *Ocean Sci. Discuss.*, *6*, 1369–1406.

Álvarez, O., C. J. González, R. Mañanes, L. López, M. Bruno, A. Izquierdo, J. Gómez-Enri, and M. Forero (2011), Analysis of short-period internal waves using wave-induced surface displacement: A 3D model approach in Algeciras Bay and the Strait of Gibraltar, *J. Geophys. Res.*, *116*, C12033, doi:10.1029/2011JC007393.

Boyer, D. L., D. B. Haidvogel, and N. Perenne (2004), Laboratory-numerical model comparisons of canyon flows: A parameter study, *J. Phys. Oceanogr.*, *34*, 1588–1609.

Boyer, D. L., X. Zhang, and N. Pérenne (2000), Laboratory observations of rotating, stratified flow in the vicinity of a submarine canyon, *Dyn. Atmos. Oceans*, *31*, 47–72.

Boyer, D. L., J. Sommeria, A. S. Mitrovic, V. K. C. Pakala, S. A. Smirnov, and D. Etling (2006), The effects of boundary turbulence on canyons flows forced by periodic along-shelf currents, *J. Phys. Oceanogr.*, *36*, 813–826.

Bray, N. A., J. Ochoa, and T. H. Kinder (1995), The role of the interface exchange through the Strait of Gibraltar, *J. Geophys. Res.*, *100*(C6), 10,755–10,776.

Bruno, M., R. Mañanes, J. J. Alonso, A. Izquierdo, L. Tejedor, and B. A. Kagan (2000), Vertical structure of the semidiurnal tidal currents at Camarinal Sill, the strait of Gibraltar, *Oceanol. Acta*, *23*(1), 15–24.

Bruno, M., J. J. Alonso, A. Cózar, J. Vidal, A. Ruiz-Cañavate, F. Echevarría, and J. Ruiz (2002), The Bowling-water phenomena at Camarinal Sill, the Strait of Gibraltar, *Deep Sea Res., Part II*, *49*, 4097–4113.

Candela, J. (1990), The barotropic tide in the Strait of Gibraltar, in *The Physical Oceanography of Sea Straits*, edited by L. J. Pratt, pp. 457–475, Kluwer, Dordrecht, Netherlands.

Candela, J., C. Winant, and A. Ruiz (1990), Tides in the Strait of Gibraltar, *J. Geophys. Res.*, *95*(C5), 7313–7335.

Candela, J., C. D. Winant, and H. L. Bryden (1989), Meteorologically forced subinertial flows through the Strait of Gibraltar, *J. Geophys. Res.*, *94*(12), 667–679.

Chioua, J., M. Bruno, A. Vázquez, M. Reyes, J. J. Gomiz, R. Mañanes, O. Álvarez, C. González, L. López, and J. Gómez-Enri (2013), Internal waves in the Strait of Gibraltar and their role in the vertical mixing processes within the Bay of Algeciras, *Estuarine Coastal Shelf Sci.*, *126*, 70–86.

De Buen, R. (1924), Avance al estudio de la oceanografía de la Bahía de Algeciras, *Bol. Pescas*, *9*(89), 1–32.

Dorman, C. E., R. C. Beardsley, and R. Limeburner (1995), Winds in the Strait of Gibraltar, *Q. J. R. Meteorol. Soc.*, *121*(528), 1903–1921.

Elliot, A. J., K. M. Ellis, and N. M. Lynn (2003), Baroclinic tidal currents in the Gareloch, Scotland, *Estuarine Coastal Shelf Sci.*, *58*, 107–116.

Environmental Quality Plan for the Campo de Gibraltar Dossier (2004), Estudio de la calidad ambiental del Campo de Gibraltar, IV Informe. [Available at www2.uca.es/grup-invest/plan-campodegibraltar/.].

Foreman, M. G. G., and R. F. Henry (1989), The harmonic analysis of tidal model time series, *Adv. Water Resour.*, *12*, 109–120.

García, M. J. (2006), Estación mareográfica de Tarifa, Instituto Español de Oceanografía, Área de Medio Ambiente y Protección Ambiental. [Available at www.ieo.es/indamar/mareas/documentos/informe-estadisticas-tarifa.pdf.].

García-Lafuente, J., E. Álvarez-Fanjul, J. M. Vargas, and A. W. Ratsimandresy (2002), Subinertial variability in the flow through the Strait of Gibraltar, *J. Geophys. Res.*, *107*(C10), 3168, doi:10.1029/2001JC001104.

García-Lafuente, J., J. M. Vargas, F. Plaza, T. Sarhan, J. Candela, and B. Bascheck (2000), Tide at the eastern section of the Strait of Gibraltar, *J. Geophys. Res.*, *105*(C6), 14,197–14,213.

García-Lafuente, J., T. Sarhan, M. Vargas, J. M. Vargas, and F. Plaza (1999), Tidal motions and tidally induced fluxes through La Línea submarine canyon, western Alboran Sea, *J. Geophys. Res.*, *104*(C2), 3109–3119.

García-Lafuente, J. M. (1986), Variabilidad del nivel del mar en el Estrecho de Gibraltar: Mareas y oscilaciones residuals, PhD thesis, Instituto Espaol de Oceanografía, Fuengirola, Malaga, Spain.

Gill, A. E. (1982), *Atmosphere-Ocean Dynamics*, Academic, San Diego, Calif.

Haidvogel, D. B. (2005), Cross-shelf exchange driven by oscillatory barotropic currents at an idealized coastal canyon, *J. Phys. Oceanogr.*, *35*, 1054–1067.

Hickey, B. M. (1995), Coastal submarine canyons, in *Topographic Effects in the Ocean*, edited by P. Müller and D. Henderson, pp. 95–110, Sch. of Ocean and the Earth Sci. and Technol., Manoa.

Hickey, B. (1997), The response of a steep-sided, narrow canyon to time-variable wind forcing, *J. Phys. Oceanogr.*, *27*, 697–726.

Izquierdo, A., L. Tejedor, D. V. Sein, O. Backhaus, P. Brandt, A. Rubino, and B. A. Kagan (2001), Control variability and internal bore evolution in the Strait of Gibraltar: A 2-D two-layer model study, *Estuarine Coastal Shelf Sci.*, *53*, 637–651.

Kämpf, J. (2007), On the interaction of time-variable flows with a shelf-break canyon, *J. Phys. Oceanogr.*, *39*, 248–260, doi:10.1175/2008JPO3753.1.

Lacombe, H., and C. Richez (1982), The regime of the Strait of Gibraltar, *Elsevier Oceanogr. Ser. 34*, 13–73.

Lee, I. H., R. C. Lien, J. T. Liu, and W. S. Chuang (2009), Turbulent mixing and internal tides in Gaoping (Kaoping) Submarine Canyon, Taiwan, *J. Mar. Syst.*, *76*(4), 383–369, doi:10.1016/j.jmarsys.2007.12.011.

Mañanes, R., M. Bruno, J. J. Alonso, B. Fraguela, and L. Tejedor (1998), Non-linear interaction between tidal and subinertial flows in the Strait of Gibraltar, *Oceanol. Acta*, *21*(1), 33–46.

Mellor, G. L. (1996), *Users Guide for a Three-Dimensional, Primitive Equation, Numerical Ocean Model*, Prog. Atmos. and Ocean Sci., Princeton University.

Mellor, G. L., and T. Yamada (1982), Development of a turbulence closure model for geophysical fluid problems, *Rev. Geophys. Space Phys.*, *20*(4), 851–875.

Pairaud, I. L., F. Lyard, F. Auclair, T. Letellier, and P. Marsaleix (2008), Dynamics of the semi-diurnal and quarter-diurnal internal tides in the Bay of Biscay. Part 1: Barotropic tides, *Cont. Shelf Res.*, *28*, 1294–1315.

Palmer, M. R. (2010), The modification of current ellipses by stratification in the Liverpool Bay ROFI, *Ocean Dyn.*, *60*, 219–226, doi:10.1007/s10236-009-0246-x.

Pingree, R. D., and L. Maddock (1979), Tidal flow around an island with a regularly sloping bottom topography, *J. Mar. Biol. Assoc. U. K.*, *59*(03), 699–710.

Quaresma, L. S., and A. Pichon (2013), Modelling the barotropic tide along the West-Iberian margin, *J. Mar. Syst.*, *109–110*, S3–S25, doi:10.1016/j.jmarsys.2011.09.016.

Richtmyer, R. D., and K. W. Morton (1967), *Difference Methods for Initial-Value Problems*, Interscience, New York.

Sánchez-Román, A., F. Criado-Aldeanueva, J. García-Lafuente, and J. C. Sánchez (2008), Vertical structure of tidal currents over Espartel and Camarinal sills, Strait of Gibraltar, *J. Mar. Syst.*, *74*(1–2), 120–133, doi:10.1016/j.jmarsys.2007.11.00.

Sannino, G., A. Carillo, and V. Artale (2007), Three-layer view of transports and hydraulics in the strait of Gibraltar: A three-dimensional model study, *J. Geophys. Res.*, *112*, C03010, doi:10.1029/2006JC003717.

Signell, R. P., and W. R. Geyer (1991), Transient eddy formation around headlands, *J. Geophys. Res.*, *96*(C2), 2561–2576.

Skliris, N. S. Sofianos, and A. Lascaratos (2007), Hydrological changes in the Mediterranean Sea in relation to changes in the freshwater budget: A numerical modelling, *J. Mar. Syst.*, *65*, 400–416, doi:10.1016/j.jmarsys.2006.01.015.

Tee, K. T. (1976), Tide-induced residual current, a 2-D nonlinear numerical tidal model, *J. Mar. Res.*, *34*, 603–628.

Tejedor, L., A. Izquierdo, and D. V. Sein (1999), Simulation of the semi-diurnal tides in the Strait of Gibraltar, *J. Geophys. Res.*, *104*(C6), 13,541–13,557.

Tejedor, L., A. Izquierdo, D. V. Sein, and B. A. Kagan (1998) Tides and tidal energetics of the Strait of Gibraltar: A modelling approach, *Tectonophysics*, *294*(3–4), 333–347.

Tsimplis, M. N. (2000), Vertical structure of tidal currents over Camarinal Sill at the Strait of Gibraltar, *J. Geophys. Res.*, *105*(C8), 16,223–16,239.

Tsimplis, M., R. Proctor, and R. Flather (1995), A two-dimensional tidal model for the Mediterranean Sea, *J. Geophys. Res.*, *100*(C8), 16,223–16,239.

Vargas, J., J. García-Lafuente, J. Candela, and A. Sánchez (2006), Fortnightly and monthly variability of the exchange through the Strait of Gibraltar, *Prog. Oceanogr.*, *70*(2–4), 466–485, doi:10.1016/j.pocean.2006.07.001.

Vázquez, A., M. Bruno, A. Izquierdo, D. Macías, and A. Ruiz-Cañavate (2008), Meteorologically forced subinertial flows and internal wave generation at the main sill of the Strait of Gibraltar, *Deep Sea Res., Part I*, *55*, 1277–1283, doi:10.1016/j.dsr.2008.05.008.

Waterhouse, A. F., S. E. Allen, and A. W. Bowie (2009), Upwelling flow dynamics in long canyons at low Rossby number, *J. Geophys. Res.*, *114*, C05504, doi:10.1029/2008JC004956.

World Ocean Circulation Experiment (1990–2002) [Available at: http://woce.nodc.noaa.gov.].